Core-Spun Carbon Nanotube Yarn Supercapacitors for Wearable Electronic Textiles

Daohong Zhang,[†,‡] Menghe Miao,[†,*] Haitao Niu,[§] and Zhixiang Wei[⊥]

[†]CSIRO Materials Science and Engineering, P.O. Box 21, Belmont, Victoria 3216, Australia, [‡]Key Laboratory of Catalysis and Materials Science of the State Ethnic Affairs Commission & Ministry of Education, South-Central University for Nationalities, Wuhan, Hubei Province 430074, China, [§]Institute for Frontier Materials, Deakin University, Geelong, Victoria 3220, Australia, and [⊥]National Center for Nanoscience and Technology, Beijing 100190, P. R. China

ABSTRACT Linear (fiber or yarn) supercapacitors have demonstrated remarkable cyclic electrochemical performance as power source for wearable electronic textiles. The challenges are, first, to scale up the linear supercapacitors to a length that is suitable for textile manufacturing while their electrochemical performance is maintained or preferably further improved and, second, to develop practical, continuous production technology for these linear supercapacitors. Here, we present a core/sheath structured carbon nanotube yarn architecture and a method for one-step continuous spinning of the core/sheath yarn that can be made into long linear supercapacitors. In the core/sheath structured yarn, the carbon nanotubes form a thin surface layer around a highly conductive metal filament core, which serves as current collector so that charges produced on the active materials along the length of the supercapacitor are transported efficiently, resulting in significant improvement in electrochemical performance and scale up of the supercapacitor length. The long, strong, and flexible threadlike supercapacitor is suitable for production of large-size fabrics for wearable electronic applications.

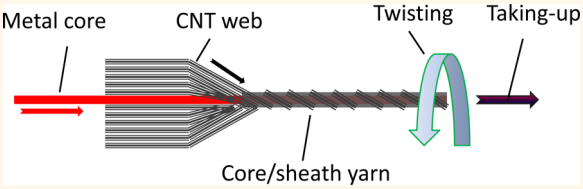

KEYWORDS: supercapacitors · carbon nanotubes · core yarns · current collectors · nanotechnology

Flexible batteries and supercapacitors are desirable power sources for lightweight, portable, and wearable electronics that have become symbolic of modern life. These flexible energy storage devices may be of one-dimensional (1D, or linear) or two-dimensional (2D, or planar) architectures.[1−3] Planar supercapacitors are mostly built on metal sheets, plastic films, papers, and textile fabric substrates.[1,2,4,5] After impermeable layers of active materials, separation membranes, and current collectors are deposited, the 2D supercapacitors often become quite bulky, their flexibility deteriorates considerably, and the resulting supercapacitors lose their permeability to ambient air and perspiration moisture, all of which are essential for wearer comfort.[6−9] These problems will become major concerns if the devices cover a large area of the clothing system.

In comparison, linear energy storage devices may be woven or knitted, alone or in combination with textile yarns, into fabrics that are both robust and comfortable to wear.[10−13] The freedom for body movement (fabrics can be bent or folded easily) and permeability to air and moisture (transport of body sweat vapor) in woven and knitted fabrics originate from their interlaced structures in which the constituent yarns are free to move relative to each other, and there are through-thickness holes formed between the constituent yarns. The fineness of linear supercapacitors range from much finer than extrafine count textile yarns used in high quality handkerchiefs[10,11] to very coarse count yarns used in winter sweaters and blankets.[14]

Linear supercapacitor devices can be built on linear substrates such as metal wires,[7,11,14−16] plastic/rubber wires,[17,18] carbon fibers,[14] carbon nanofibers,[19] carbon nanotube (CNT) yarns,[7,10,11,20−23] CNT composite fibers,[11,24] graphene fibers,[25] and graphene composite fibers.[26] These substrates serve as the reinforcement as well as the charge collector for the active materials. Nonconductive substrates may be coated with conductive (*e.g.*, metal) materials so that they can act as current collectors for active materials.[17] Active materials used in

* Address correspondence to menghe.miao@csiro.au.

Received for review January 8, 2014 and accepted April 22, 2014.

Published online April 22, 2014
10.1021/nn5001386

linear supercapacitors may be carbon nanoparticles,[14,16,24] metal oxides,[11,12,17,23] and conducting polymers.[10,13,21] Metal oxides and conducting polymers are high performance materials because of their high pseudocapacitance and the capability to charge and discharge at high rates.[27−31] The electrochemical performance of pseudocapacitance materials can be further improved when they are made into nanowires, for example, polyaniline nanowires and ZnO nanowires.[17,31]

Carbon nanotubes are electrical double-layer capacitor (EDLC) materials on their own. Vertically aligned CNT arrays (CNT forests) have an ideal mesoporous structure for high electrolyte accessibility.[32−34] Carbon nanotube yarns spun from CNT forests have excellent textile properties (strong and flexible),[35] and have been a popular substrate for constructing linear supercapcitors.[7,10,11,20−23] When used as a substrate, their high mechanical strength and stability can help obviate degradation of mechanical and electrochemical performances of conducting polymer caused by swelling and shrinking during the doping and dedoping processes.[10,36] Linear supercapacitors based on carbon nanotube yarns have demonstrated remarkable cyclic electrochemical performance over short lengths. Their performance decreases rapidly as the yarn length increases. Although carbon nanotube yarns have much higher electrical conductivity[37] than widely used pseudocapacitance materials as current collectors,[38−41] their conductivity is still 100s of times lower than that of metal wires. A key challenge is therefore to scale up them to a length that is suitable for textile manufacturing while their electrochemical performance is maintained or preferably further improved.

Here, we present an architecture that can greatly scale up the length and significantly improve the electrochemical performance of CNT yarn-based linear supercapacitors. These are achieved by embedding a very thin metal wire (monofilament) in the center of a carbon nanotube yarn. In the core/sheath structured yarn, the carbon nanotubes form a thin surface layer with high electrolyte accessibility and much shorter routes for transporting charges produced on the main active materials to the highly conductive metal core. In this way, charges stored along the length of the linear supercapacitors can be transported at very high efficiency.

Solid-state multiwalled carbon nanotube (MWCNT) forests used in this study were grown on silicon wafers using a chemical vapor deposition method.[42] The core/sheath-structured CNT yarn was manufactured on a flyer spinner, as shown in Figure 1.[35] The continuous core yarn spinning operation is explained with reference to the schematic in Figure 2. The CNTs forming the sheath are drawn from the MWCNT forest as a continuous web. The core material, which is a 25 μm diameter platinum monofilament, is pulled out

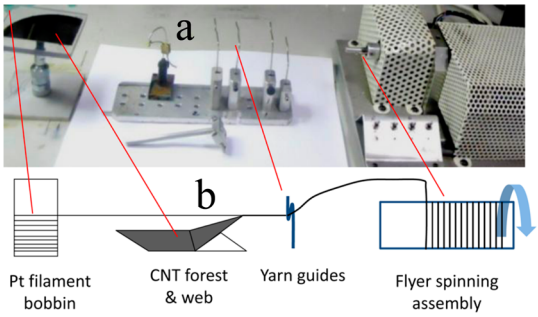

Figure 1. Continuous spinning of Pt/CNT core/sheath yarns: (a) photograph of the flyer spinner; (b) schematics of working elements.

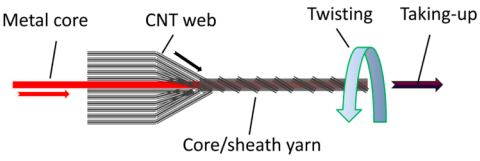

Figure 2. Schematic showing formation of the core/sheath yarn structure.

from the supply bobbin (Figure 1) to merge with the CNT web. The twisting action of the spindle at the right-hand side causes the Pt filament and the CNT web to rotate together, resulting in the wrapping of the CNT web around the filament to form a core/sheath structured yarn. The resulting core spun yarn is simultaneously collected onto the collection bobbin using the flyer-spindle assembly shown in Figure 1. Because of the very large width of the CNT web (~10 mm) in relation to the diameter of the metal filament (0.025 mm, or 25 μm), the filament is completely covered by the CNT sheath in the resultant core spun yarn, similar to the conventional core yarn spinning used by the textile industry.[43−45] The continuous core yarn spinning process was recorded on video and is included in the Supporting Information. When the spindle is run at 5000 rpm, core/sheath yarns with 5000 CNT wraps per meter can be produced continuously at a rate of 60 m/h.

RESULTS AND DISCUSSION

The electrical conductivity of the Pt filament (9.4×10^6 S/m) is 300 times higher than that of a pure CNT yarn ($\sim 3 \times 10^4$ S/m).[37] The electrical conductivity of the resulting core/sheath yarn Pt/CNT is 5.5×10^6 S/m because of the dominance of the highly conductive Pt filament. The core/sheath yarn also shows a high tensile strength (550 MPa), which is about 80% of the pure CNT yarn strength (680 MPa). This is still much higher than the strength of conventional textile yarns; for example, high-quality extrafine count combed cotton yarns have a typical tenacity (specific strength) below 30 cN/tex,[46] which translates into approximately 200 MPa.

To expose the yarn cross-sectional structures, we used a focused ion beam (FIB) to mill a pure CNT yarn and a

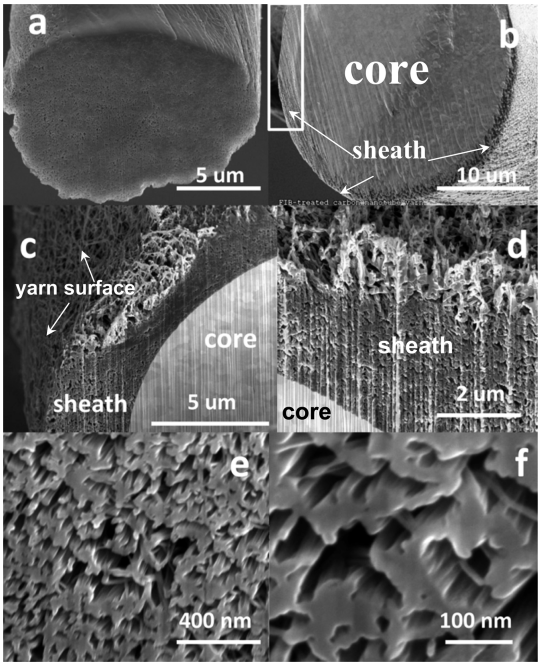

Figure 3. Yarn cross-sectional views: (a) cross-section of pure CNT yarn; (b) cross-section of Pt/CNT/PANI core/sheath yarn resulted from coarse FIB milling; (c, d) core/sheath border regions of Pt/CNT/PANI yarn after polish-milling, corresponding to the marked region in image b; (e, f) enlargements showing CNT bundles and pores between CNT bundles in the yarn cross-section.

Pt/CNT/PANI coated core/sheath yarn. The cross-sectional morphology of the pure CNT yarn is exhibited in Figure 3a, in which randomly distributed voids are visible. SEM images for the Pt/CNT/PANI core/sheath yarn taken at two stages of FIB milling are presented in Figure 3b–d. The cross-section obtained from initial coarse milling using a high beam current of 31 nA (Figure 3b) did not provide clear views in the core/sheath border region due to severe redeposition of platinum sputtering onto the newly formed sectional face. To obtain a clear sectional face, the coarse-milled section was further processed by "polish milling" at a much lower beam current (2 nA). This produced clear sectional views in the core/sheath border regions (Figure 3c,d).

There are no obvious differences between the Pt/CNT core/sheath yarn and the pure CNT yarn in terms of CNT packing observed from the sectional faces. Enlarged views in Figure 3e,f show that pores between constituent CNTs take different shapes, with the majority greater than 100 nm. These pores appear to orientate along the CNT length (following the general direction of the twist helices in the yarn) and are presumably interconnected. The SEM images in Figure 3c, d also show that the platinum filament core (bright arc segments at the lower corners of the images marked by "core") is surrounded by the CNTs in the sheath. No gaps between the CNT sheath and the Pt core could be observed. This was because the CNT web was tightly wrapped round the Pt filament under tension during spinning, resulting in compression between the two components.

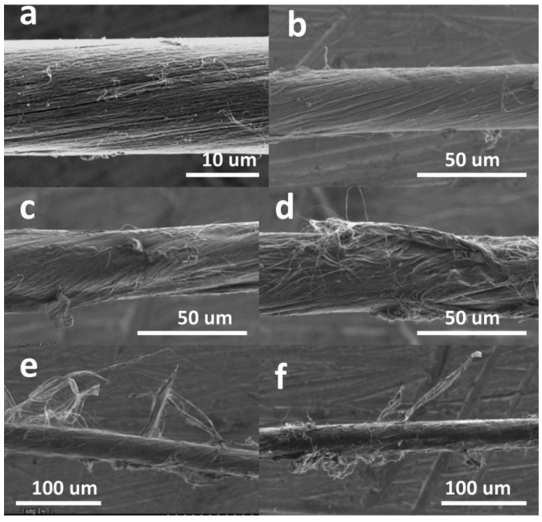

Figure 4. SEM images of CNT yarn and Pt/CNT core/sheath yarn: (a) as-spun CNT yarn; (b) as-spun Pt/CNT core/sheath yarn; (c–f) Pt/CNT core/sheath yarn after 120 rubbing actions.

The surface morphologies of CNT and Pt/CNT yarns were examined by scanning electron microscopy (SEM). The pure CNT yarn has a diameter of approximately 16 μm (Figure 4a) with well-aligned CNTs on the yarn surface. The as-spun Pt/CNT core/sheath yarn shows a diameter of about 29.5 μm with similar CNT alignment on the yarn surface (Figure 4b).

Typical textile processes require a yarn to slide over machine parts, during which the yarn bends and rubs against the parts. Such combined bending and rubbing action can be simulated by a needle-and-pin arrangement shown in Figure S1 (Supporting Information). By moving the latch needle up and down, the yarn is bent and rubbed against the needle and the pins repeatedly while under a 10 cN/tex tension based on the CNT component. The friction on the CNT sheath applied by the needle and pins tend to tear the CNT sheath off from its metal filament core, a failure mode known as sheath slippage in the textile industry.[45] The experiment provides an indication of the interfacial strength between the CNT sheath and the Pt core. SEM images of CNT/Pt core spun yarn specimens after 60 cycles of rubbing test (60 up-and-down actions, giving a total of 120 rubs) are shown in Figure 4c–f. There were no signs of sheath slippage or sheath being stripped off the Pt filament core. The rubbing action only caused some roughening of yarn surface, resulting in some CNTs being lifted up from the yarn surface. This demonstrates that the interface between the CNT sheath and the Pt core is very strong. In the final supercapacitor, the CNT sheath is protected by the polymer electrolyte coating (PVA–H_3PO_4); thus, the CNT sheath will not be rubbed against machine parts

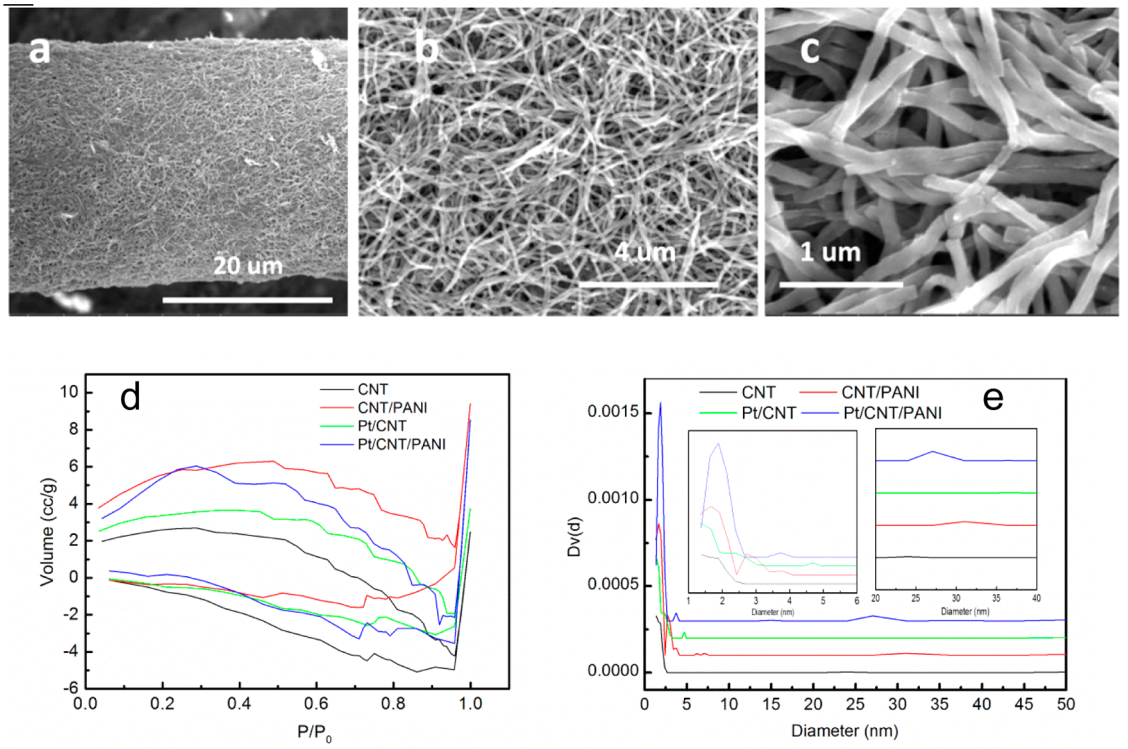

Figure 5. Yarn surface characteristics after deposition of polyaniline nanowires: (a–c) SEM images at different magnifications; (d) N_2 adsorption–desorption isotherms of CNT and Pt/CNT yarns with and without PANI nanowires; (e) mesopore diameter distributions.

directly during textile processing and CNTs will not be lifted off like the uncoated yarn shown in Figure 4c–f.

The CNT and Pt/CNT yarns were then coated in polyaniline nanowire solution synthesized using a known procedure with some minor modifications.[29,47] The coating was carried out using the continuous coating and drying line displayed in Figure S2 (Supporting Information). Coating of the relatively small amount of polyaniline nanowires (about 10 wt %) resulted in little change of yarn diameter. The polyaniline nanowires on the yarn surface in Figure 5a–c show random orientation in contrast to the vertically aligned ployaniline nanowire arrays obtained by the more sophisticated in situ deposition polymerization method reported previously.[10] The randomly orientated ployaniline nanowires obtained in this work are quite uniform in diameter (about 50 nm) but vary in length, mostly in the range from about 2 to 5 μm. The results of nitrogen adsorption–desorption experiments show that the incorporation of the polyaniline nanowires introduced mesopores of about 30 nm in dimension (Figure 5d,e) and increased the surface area and pore volume of both the CNT yarn and the Pt/CNT yarn (Table S1, Supporting Information).

The four types of yarns (CNT, Pt/CNT, CNT/PANI, and Pt/CNT/PANI) were then coated with poly(vinyl alcohol)–phosphoric acid gel electrolyte (PVA–H_3PO_4) using the continuous coating and drying line shown in Figure S2 (Supporting Information). In addition, the bare Pt filament was coated with polyaniline nanowires and PVA–H_3PO_4 to form another type of electrode, Pt/PANI. The take-up ratio of polyaniline nanowires for the Pt/PANI yarn was low due to the poor adhesion of PANI to the bare Pt filament (Figure S5, Supporting Information). After PVA–H_3PO_4 was coated, the diameter of the pure CNT yarn and CNT/PANI yarn was increased to about 24 μm, the Pt/PANI yarn to about 31 μm, and the Pt/CNT yarn and Pt/CNT/PANI yarn to about 35 μm, giving a similar PVA layer thickness of about 4–5 μm for all the yarns. These coated yarns were then folded and twisted to form five types of two-ply yarn supercapacitors using the twisting device shown in Figure S3 (Supporting Information). An optical image of a final two-ply yarn supercapacitor is shown in Figure 6a. The final two-ply yarn supercapacitor Pt/CNT/PANI has a diameter of about 70 μm (Figure 6b), which is still much finer than extrafine count textile yarns (hundreds of micrometers in diameter) so that the supercapacitor can be made into very thin fabrics on its own or normal thickness fabrics in combination with conventional textile yarns for use in wearable electronic textiles.

It is recognized in the textile industry that knitting requires highly flexible yarns. In weaving, one constituent yarn is bent over a perpendicular yarn to form a gentle arc-shaped curve. In knitting, the yarn is folded on its own back to form a narrow heart-shaped loop. To demonstrate the high flexibility and strength of

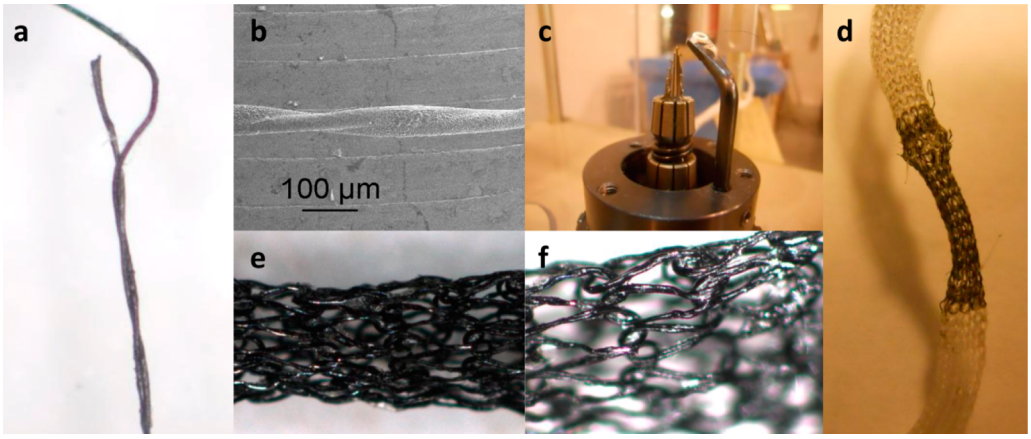

Figure 6. Production of a weft-knit tubular fabric from the Pt/CNT/PANI two-ply yarn supercapacitor: (a) optical image of two-ply yarn supercapacitor; (b) SEM image of the Pt/CNT/PANI two-ply yarn supercapacitor; (c) 10-needle fine gauge weft-knitting machine used to produce the tubular fabric; (d) knitted tubular fabric containing the Pt/CNT/PANI supercapacitor (middle black section) and a nylon monofilament (semitransparent end sections); (e, f) optical microscope images showing loop structure of the Pt/CNT/PANI supercapacitor in the knitted tubular fabric.

the linear supercapacitor, a half-meter long Pt/CNT/PANI two-ply yarn supercapacitor was knitted on a fine gauge circular weft-knitting machine as shown in Figure 6c. The linear supercapacitor forms the middle section of the tube shown in Figure 6d. The successive sections of the tube were knitted from a nylon monofilament to form a long tubular structure of about 2 mm in diameter. The optical microscope images in Figure 6e,f show the loop structure of the supercapacitor in the tubular fabric at two different magnifications.

The five types of two-ply yarns are symmetric two-electrode solid-state supercapacitors with the two singles yarns as the two electrodes and the PVA−H_3PO_4 gel coating as both electrolyte and separator. The electrochemical properties of these supercapacitors were characterized by cyclic voltammetry (CV), galvanostatic charge/discharge, and electrochemical impedance spectroscopy (EIS). Figure 7a shows the CV curves of these two-ply yarn supecapacitors. The pure CNT and Pt/CNT yarn supercapacitors show near-rectangular shape CV curves, which are typical of electrochemical double-layer supercapacitors.[48] The Pt/PANI, CNT/PANI, and Pt/CNT/PANI yarn supercapacitors demonstrate double-redox peaks which are characteristic of PANI materials.[49] The incorporation of Pt filament core in CNT yarn and the coating of PANI increased the current density as indicated by the areas of their CV windows. Figure 7b presents the CV curves of the Pt/CNT/PANI yarn supercapacitor at different scanning rates. The galvanostatic charge/discharge curves in Figure 7c show that the incorporation of the Pt filament core extended the charge/discharge times of the CNT-containing supercapacitors significantly.

The specific capacitances of the five types of two-ply yarn supercapacitors are plotted against the scanning rate in Figure 7d−f. Overall, the Pt/CNT/PANI yarn supercapacitor showed 3- to 9-fold increases in gravimetric capacitance over the pure CNT/PANI-, Pt/CNT-, and CNT yarn-based supercapacitors, respectively. The Pt/PANI supercapacitor showed a gravimetric capacitance lower than that of the Pt/CNT/PANI supercapacitor but higher than the other three types of supercapcitors. The length and areal capacitances of the Pt/PANI supercapacitor were similar to that of the CNT/PANI supercapacitor. The gravimetric capacitance 86.2 F g^{-1} for the Pt/CNT/PANI two-ply yarn supercapacitor measured at the scanning rate of 5 mV s^{-1} is equivalent to an area capacitance of 52.5 mF cm^{-2} (Figure 7f), which is significantly higher than the areal capacitances of many recently reported linear supercapacitors.[10,14−18,22,23] The equivalent capacitance based on supercapacitor length is 241.3 μF cm^{-1} (Figure 7e). Although a useful measure for linear supercapacitors, the length-based capacitance is largely biased toward thick supercapacitors which can carry a large quantity of active materials in a unit length.

Figure 7g summarizes the individual and combined effects of PANI nanowires and Pt filament on the capacitance of the CNT yarn at the scanning rate of 5 mV s^{-1}. The average individual effects were 41.2 F g^{-1} for PANI and 35.0 F g^{-1} for Pt filament, respectively, giving a combined effect of 76.1 F g^{-1}. The effect of incorporating Pt filament was seven times greater for the CNT/PANI yarn supercapacitor (61.7 F g^{-1}) than for the pure CNT yarn supercapacitor (8.2 F g^{-1}). By incorporating the Pt filament, the energy density and power density of the supercapacitor at scan rate 100 mV s^{-1} were increased from 13.63 Wh kg^{-1} to 35.27 Wh kg^{-1} and from 2.39 kW kg^{-1} to 10.69 kW kg^{-1}, respectively.

These four types of supercapacitors were further characterized using electrochemical impedance spectroscopy (EIS). The Nyquist plots in Figure 7h departed from each other at the low frequency range (higher ends of the curves), with the imaginary components of impedance following a ranking order opposite to that

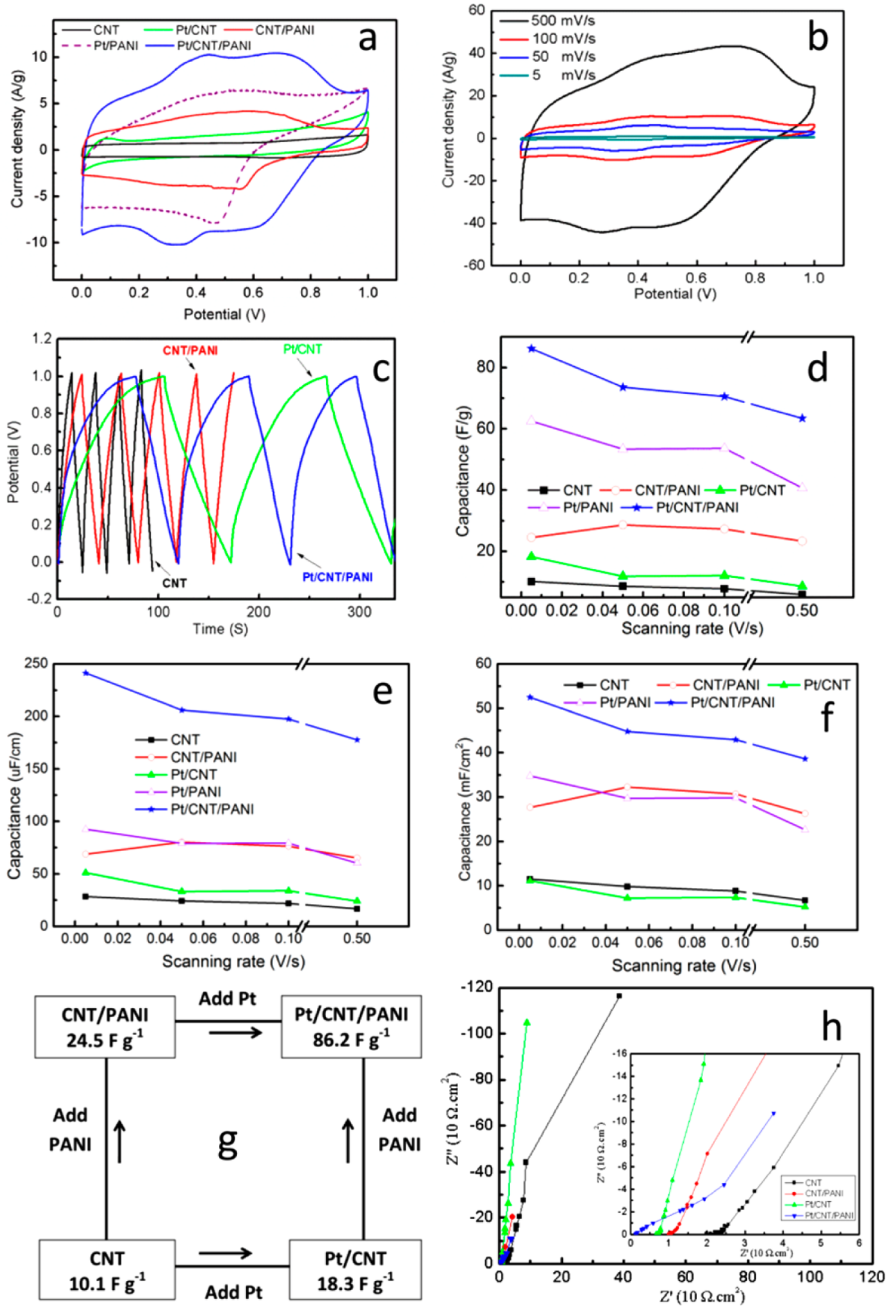

Figure 7. Electrochemical properties of two-ply yarn supercapacitors: (a) cyclic voltammograms of the different types of supercapacitors at the same scanning rate of 100 mV s^{-1}; (b) cyclic voltammograms of the Pt/CNT/PANI supercapacitor at different scanning rates; (c) galvanostatic charge/discharge curves of the different types of supercapacitors; (d) gravimetric capacitances of the different types of supercapacitors as a function of scanning rate; (e) length-based capacitances as a function of scanning rate; (f) areal capacitances as a function of scanning rate; (g) effects of polyaniline nanowire deposition and Pt filament core on the gravimetric capacitance of the two-ply yarn supercapacitors; (h) electrochemical impedance spectra (0.01 Hz−500 kHz).

of the specific capacitances in Figure 7d. The inset in Figure 7h shows the impedances of the four supercapacitors at the high frequency range (lower ends of the curves). The *x*-intercept of the Nyquist plot represents the equivalent series resistance (ESR) that corresponds to charge transport resistance for two-electrode supercapacitor.[10] The inset results show that incorporating the Pt filament core has reduced the ESR of the supercapacitors significantly. The Pt/CNT yarn supercapacitor has a third of the ESR of the pure CNT yarn supercapacitor, and the Pt/CNT/PANI supercapacitor has a ESR that is 1 order of magnitude smaller than that of the CNT/PANI yarn supercapacitor.

Figure 8a shows the size effect of the CNT, CNT/PANI, and Pt/CNT/PANI two-ply yarn supercapacitors. Without the Pt filament core, the specific capacitances of the pure CNT and CNT/PANI supercapacitors diminish very quickly with the increase of supercapacitor length.

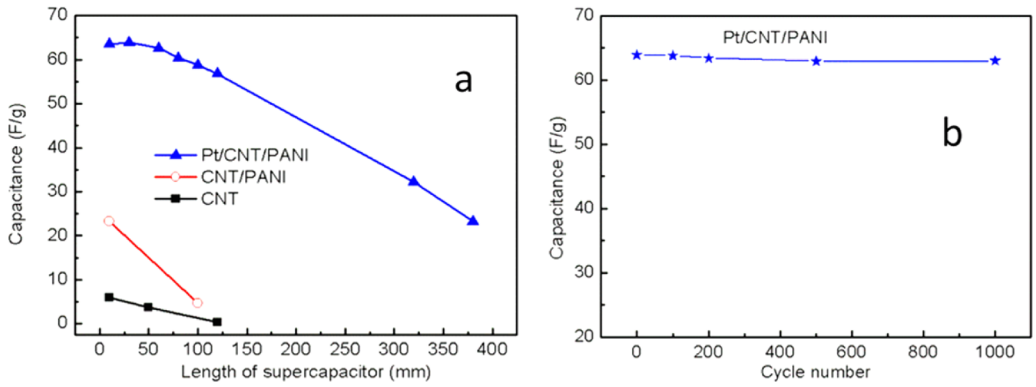

Figure 8. Capacitance retention: (a) size effects on different supercapacitors at a constant scanning rate 500 mV s^{-1}; (b) effect of repeated folding-unfolding actions on the capacitance of Pt/CNT/PANI two-ply yarn supercapacitor.

The capacitances of these two supercapacitors at 100 mm length dropped to less than 20% of their base values at 10 mm. In comparison, the Pt/CNT/PANI supercapacitor maintained 93% of its base capacitance at 10 mm when its length was increased to 100 mm, and 51% when its length was further increased to 320 mm. This means that the Pt/CNT/PANI two-ply yarn supercapacitor may be used as weft to produce foot-wide woven fabrics.

Textile materials experience many cycles of bending actions during fabrication and end use. The most severe form of bending action is repeated folding and unfolding (flattening). As part of a wearable electronic system, two-ply yarn supercapacitors must maintain their electrochemical performance after a large number of folding−unfolding cycles. As shown in Figure 8b, the capacitance of the Pt/CNT/PANI supercapacitor had little change after being subjected to 1000 cycles of folding and unfolding.

The above results suggest that the Pt/CNT core/sheath yarn architecture played an important role in improving the capacitance and up-scaling of the two-ply yarn supercapacitors. CNT yarns have a porous structure which favors ionic motion and rate performance of electrodes.[9] However, pure CNT yarns are not highly conductive, with its electrical conductivity far below metals. Charges generated on the active materials (PANI nanowires and the CNTs) in the electrode have to cross a very large number of CNT-CNT boundaries to be transported along the yarn length, resulting in low efficiency.[7] With the incorporation of a metal filament core, charges generated in the electrode only need to cross a few CNT boundaries through the thickness of the CNT sheath (2−3 μm) to reach the highly conductive metal core. The metal filament core serves as a super highway that collects the charges generated at every position of the electrode and transports them efficiently along the yarn length. The CNT sheath provides a porous substrate with which the PANI nanowires can form an effective interface, as well as provides the strength and flexibility to overcome fatigue of the high performance PANI polymer caused by repeated mechanical bending and due to swelling and shrinking during cyclic charge and discharge.

CONCLUSION

We have reported a new carbon nanotube yarn structure and its suitability for application in linear supercapacitors. The new yarn consists of a high conductivity metal filament coaxially embedded in a layer of carbon nanotubes and can be manufactured by a continuous core yarn spinning method. The strong and flexible core/sheath structured yarn can be plied together to form a two-ply yarn supercapacitor on its own or used as substrate for high performance pseudocapacitance materials. In the two-ply yarn supercapacitors, the metal filament core serves as current collector to provide a super highway for transportation of charges generated along the length of two-ply yarn supercapacitor, leading to significant increases in energy and power storage capacities. The new architecture enables the length of the supercapacitor to be up-scaled dramatically. Tensile test, flexing test, and machine knitting trial show that the two-ply yarn supercapacitor is highly flexible and robust as high performance power source for wearable electronic devices.

METHODS

Production of As-Spun Carbon Nanotube Yarns. CNT forests were grown on silicon wafer substrates bearing a thermal oxide layer and iron catalyst coating using chemical vapor deposition (CVD) of acetylene in helium. The synthesis procedures had been optimized as reported previously.[42] The resulting CNTs had 7 ± 2 walls with an outer diameter of 10 nm and an inner diameter of approximately 4 nm. The length of the CNTs was approximately 350 μm by measuring the height of the forests.

The core/sheath Pt/CNT yarn is manufactured using the flyer-spinner shown in Figure 1.[35] The CNT yarns were spun to a twist level of 5000 turns per meter using a spindle speed of 5000 rpm.

Preparation of Polyaniline Nanowire Solution. Polyaniline nanowires were synthesized using a reported procedure[47] with some

minor modifications. Aniline and potassium biiodate ($KH(IO_3)$), were dissolved at concentrations of 0.1 and 0.0125 M in 1 M HCl, respectively. Aniline solution (36 mL), 40 mL of $KH(IO_3)$ solution, and 1 mL of sodium hypochlorite solution (wt 5%, NaClO) were mixed and kept undisturbed at room temperature for 2.5 h. The resulting solution was centrifuged, followed by removing the supernatant. HCl (1 M) solutions were added to redissolve the synthesized PANI. After three cycles of centrifugation, the PANI nanowire solution was obtained.

Preparation of PVA−H_3PO_4 Gel. Hydrolyzed poly(vinyl alcohol) (PVA) (98−99%) with average molecular weight of 57000−66000 was supplied by Alfa Aesar. H_3PO_4 (0.8 g) (analytical grade) was added to 10 mL of deionized water with vigorous stirring, and then 1 g of PVA powder was added. The solution was heated steadily to 90 °C under vigorous stirring until the solution became clear to form the PVA−H_3PO_4 gel.

Preparation of Two-Ply Yarn Supercapacitors. Coating of PANI and PVA−H_3PO_4 gel was carried out using a home-built continuous coating line, displayed as Figure S1 in the Supporting Information. The coating line includes a pigtail-shaped reservoir for holding liquid, an electrical heating unit for drying, and an electrical motor for controlling yarn throughput speed. The liquid take-up rate and uniformity are controlled by adjusting the motor speed. Large adjustments of liquid take-up rate can be achieved by varying the viscosity of the polymer solution.

Two identical yarns were twisted together to form a two-ply yarn supercapacitor using the twisting device shown in Figure S2 (Supporting Information).

Focused Ion Beam Milling. An FEI high-resolution dual-beam Helios 600 focused ion beam (FIB) equipped with a SEM was used to form cross-sections through the CNT yarns and to take yarn cross-sectional images. The electron and ion beams intersect at a 52° angle at a coincident point near the sample surface, allowing immediate SEM imaging of the FIB-milled surface. Initially, the milling was performed with a 31 nA, 30 kV Gallium beam. The CNT sheath in the cross-section was covered by redeposition of platinum sputtering due to the high beam current. To obtained a clear image of the core/sheath yarn cross-section, a sectional surface prepared by high beam current was further treated by "polish milling" using a low beam current (2 nA). This gave a clear sectional view of the core/sheath structure.

Measurement of Linear Density. Linear density in tex (1 tex = 1 mg/m = 1 μg/mm) was determined by weighing a 100 mm length of the linear material (platinum filament, as-spun CNT yarn, Pt/CNT yarn or their coated yarns) on a high-sensitivity Mettler Toledo Xp2U Ultra Micro Balance. The linear density values were then used to calculate mass ratios of the constituent parts in the resultant yarns.

Tensile Testing. Yarn tensile tests were conducted using a Chatillon tensile testing machine equipped with a laser diffraction system for yarn diameter measurement as described previously.[50] Each specimen was attached to a paper handling frame using PVA adhesive. The testing gauge length was 10 mm. At least five specimens from each sample were tested and the average results were reported.

Strength of Pt/CNT Interface. A 3-pin device as shown in Figure S1 (Supporting Information) was constructed to test the robustness of the sheath/core interface of the Pt/CNT core spun yarn under cyclic bending and rubbing actions. One end of the yarn is tied to the fixed pin 1 and the other end is tied to a weight to provide a tension of 10 cN/tex based on the CNT sheath. When the latch needle moves up and down, the yarn is rubbed against the other three fixed pins 2, 3, and 4. Two rubs are applied to the yarn sample as the needle moves one up-and-down cycle. The CNT/Pt core spun yarns were tested for up to 60 cycles (120 rubbing actions). The rubbed areas of the yarn were then examined in SEM.

Electrical Conductivity. Electrical conductivity of CNT yarns were measured using a four-probe method.[37] The electrical resistances of CNT yarn specimens were measured at a fixed span length of 50 mm. A constant tension was applied to the yarn specimen during the measurement by hanging a mass on each end of the specimen.

Electrochemical Characterization. Cyclic voltammetry (CV), galvanostatic charge/discharge, and electrochemical impedance spectroscopy (EIS) were performed on a bipotentiostat electrochemical workstation (700D, CH Instruments) using a two-electrode configuration. Short length supercapacitors (10−50 mm) were mounted on a paper frame and connected to the instrument for measurement. Long supercapacitors (up to 380 mm) were wrapped on a tube with two ends mounted on a paper frame connector, as shown in Figure S3 (Supporting Information). Gravimetric capacitances of the supercapacitors were derived using the formula

$$C = \frac{1}{wv(V_c - V_a)} \int_{V_a}^{V_c} I(V)\mathrm{d}V \qquad (1)$$

where C is specific capacitance (F g^{-1}), w is the mass of active constituents in the working electrode (g), v is the scanning rate (V/S), $V_c - V_a$ is the potential window (V), and $I(V)$ is the current density. The mass of the active constituents (CNT and PANI) was calculated by subtracting the linear density of the platinum filament from the linear density of the Pt/CNT/PANI yarn. Specific areal capacitance was calculated by replacing w in the above equation with the surface area of the working electrode A (cm^2): $A = \pi dl$, where d is the yarn diameter in cm and l is the length of the electrode in cm.

Nitrogen Adsorption−Desorption Experiments. N_2 adsorption−desorption experiments were conducted at −196 °C with a Quantachrome Autosorb-1-C-MS. The mesopore size distributions were obtained from the desorption branches of the isotherms using the Barrett−Joyner−Halenda (BJH) method.

Conflict of Interest: The authors declare no competing financial interest.

Supporting Information Available: Photographic images of preparation and testing equipment; video of core−sheath yarn spinning. This material is available free of charge *via* the Internet at http://pubs.acs.org.

Acknowledgment. We thank the following colleagues for their assistance: A. van de Meene, Melbourne Centre for Nanofabrication, and C. P. Huynh, P. Hewitt, M. Pate, and C. Veitch, CSIRO Materials Science and Engineering. D.Z. acknowledges the China Scholarship Council for granting a visiting scholarship that enabled him to carry out this work at CSIRO in Australia.

REFERENCES AND NOTES

1. Zhi, M.; Xiang, C.; Li, J.; Li, M.; Wu, N. Nanostructured Carbon−Metal Oxide Composite Electrodes for Supercapacitors: A Review. *Nanoscale* **2013**, *5*, 72–88.
2. Cai, X.; Peng, M.; Yu, X.; Fu, Y.; Zou, D. Flexible Planar/Fiber-Architectured Supercapacitors for Wearable Energy Storage. *J. Mater. Chem. C* **2014**, *2*), 1184–1200.
3. Jost, K.; Dion, G.; Gogotsi, Y. Textile Energy Storage in Perspective. *J. Mater. Chem. A* **2014**, 10.1039/C4TA00203B.
4. Nguyen, T. H.; Fraiwan, A.; Choi, S. Paper-Based Batteries: A Review. *Biosens. Bioelectron.* **2014**, *54*, 640–649.
5. Jost, K.; Stenger, D.; Perez, C. R.; McDonough, J. K.; Lian, K.; Gogotsi, Y.; Dion, G. Knitted and Screen Printed Carbon-Fiber Supercapacitors for Applications in Wearable Electronics. *Energy Environ. Sci.* **2013**, *6*, 2698–2705.
6. Dai, L.; Chang, D. W.; Baek, J.-B.; Lu, W. Carbon Nanomaterials for Advanced Energy Conversion and Storage. *Small* **2012**, *8*, 1130–1166.
7. Ren, J.; Li, L.; Chen, C.; Chen, X.; Cai, Z.; Qiu, L.; Wang, Y.; Zhu, X.; Peng, H. Twisting Carbon Nanotube Fibers for Both Wire-Shaped Micro-Supercapacitor and Micro-Battery. *Adv. Mater.* **2013**, *25*, 1155–1159.
8. Hu, L.; Wu, H.; La Mantia, F.; Yang, Y.; Cui, Y. Thin, Flexible Secondary Li-Ion Paper Batteries. *ACS Nano* **2010**, *4*, 5843–5848.
9. Zhang, H.; Cao, G.; Wang, Z.; Yang, Y.; Shi, Z.; Gu, Z. Tube-Covering-Tube Nanostructured Polyaniline/Carbon Nanotube Array Composite Electrode with High Capacitance and Superior Rate Performance as Well as Good Cycling Stability. *Electrochem. Commun.* **2008**, *10*, 1056–1059.

10. Wang, K.; Meng, Q.; Zhang, Y.; Wei, Z.; Miao, M. High-Performance Two-Ply Yarn Supercapacitors Based on Carbon Nanotubes and Polyaniline Nanowire Arrays. *Adv. Mater.* **2013**, *25*, 1494–1498.
11. Lee, J. A.; Shin, M. K.; Kim, S. H.; Cho, H. U.; Spinks, G. M.; Wallace, G. G.; Lima, M. D.; Lepró, X.; Kozlov, M. E.; Baughman, R. H.; et al. Ultrafast Charge and Discharge Biscrolled Yarn Supercapacitors for Textiles and Microdevices. *Nat. Commun.* **2013**, *4*, 1970.
12. Su, F.; Miao, M. Asymmetric Carbon Nanotube−MnO_2 Two-Ply Yarn Supercapacitors for Wearable Electronics. *Nanotechnology* **2014**, *25*, 135401.
13. Su, F.; Miao, M. Flexible, High Performance Two-Ply Yarn Supercapacitors Based on Irradiated Carbon Nanotube Yarn and PEDOT/PSS. *Electrochim. Acta* **2014**, *127*, 433–438.
14. Fu, Y.; Cai, X.; Wu, H.; Lv, Z.; Hou, S.; Peng, M.; Yu, X.; Zou, D. Fiber Supercapacitors Utilizing Pen Ink for Flexible/Wearable Energy Storage. *Adv. Mater.* **2012**, *24*, 5713–5718.
15. Li, Y.; Sheng, K.; Yuan, W.; Shi, G.; High-Performance, A. Flexible Fibre-Shaped Electrochemical Capacitor Based on Electrochemically Reduced Graphene Oxide. *Chem. Commun.* **2013**, *49*, 291–293.
16. Harrison, D.; Qiu, F.; Fyson, J.; Xu, Y.; Evans, P.; Southee, D. A Coaxial Single Fibre Supercapacitor for Energy Storage. *Phys. Chem. Chem. Phys.* **2013**, *15*, 12215–12219.
17. Bae, J.; Song, M. K.; Park, Y. J.; Kim, J. M.; Liu, M.; Wang, Z. L. Fiber Supercapacitors Made of Nanowire-Fiber Hybrid Structures for Wearable/Flexible Energy Storage. *Angew. Chem., Int. Ed.* **2011**, *50*, 1683–1687.
18. Yang, Z.; Deng, J.; Chen, X.; Ren, J.; Peng, H. A Highly Stretchable, Fiber-Shaped Supercapacitor. *Angew. Chem., Int. Ed.* **2013**, *52*, 13453–13457.
19. Le, V. T.; Kim, H.; Ghosh, A.; Kim, J.; Chang, J.; Vu, Q. A.; Pham, D. T.; Lee, J.-H.; Kim, S.-W.; Lee, Y. H. Coaxial Fiber Supercapacitor Using All-Carbon Material Electrodes. *ACS Nano* **2013**, *7*, 5940–5947.
20. Foroughi, J.; Spinks, G. M.; Ghorbani, S. R.; Kozlov, M. E.; Safaei, F.; Peleckis, G.; Wallace, G. G.; Baughman, R. H. Preparation and Characterization of Hybrid Conducting Polymer-Carbon Nanotube Yarn. *Nanoscale* **2012**, *4*, 940–945.
21. Cai, Z.; Li, L.; Ren, J.; Qiu, L.; Lin, H.; Peng, H. Flexible, Weavable and Efficient Microsupercapacitor Wires Based on Polyaniline Composite Fibers Incorporated with Aligned Carbon Nanotubes. *J. Mater. Chem. A* **2013**, *1*, 258–261.
22. Chen, X.; Qiu, L.; Ren, J.; Guan, G.; Lin, H.; Zhang, Z.; Chen, P.; Wang, Y.; Peng, H. Novel Electric Double-Layer Capacitor with a Coaxial Fiber Structure. *Adv. Mater.* **2013**, *25*, 6436–6441.
23. Xu, P.; Gu, T.; Cao, Z.; Wei, B.; Yu, J.; Li, F.; Byun, J.-H.; Lu, W.; Li, Q.; Chou, T.-W. Carbon Nanotube Fiber Based Stretchable Wire-Shaped Supercapacitors. *Adv. Energy Mater.* **2014**, *4*, 1300759.
24. Ren, J.; Bai, W.; Guan, G.; Zhang, Y.; Peng, H. Flexible and Weaveable Capacitor Wire Based on a Carbon Nanocomposite Fiber. *Adv. Mater.* **2013**, *25*, 5965–5970.
25. Meng, Y.; Zhao, Y.; Hu, C.; Cheng, H.; Hu, Y.; Zhang, Z.; Shi, G.; Qu, L. All-Graphene Core-Sheath Microfibers for All-Solid-State, Stretchable Fibriform Supercapacitors and Wearable Electronic Textiles. *Adv. Mater.* **2013**, *25*, 2326–2331.
26. Cheng, H.; Dong, Z.; Hu, C.; Zhao, Y.; Hu, Y.; Qu, L.; Chen, N.; Dai, L. Textile Electrodes Woven by Carbon Nanotube-Graphene Hybrid Fibers for Flexible Electrochemical Capacitors. *Nanoscale* **2013**, *5*, 3428–3434.
27. Xu, J.; Wang, K.; Zu, S.-Z.; Han, B.-H.; Wei, Z. Hierarchical Nanocomposites of Polyaniline Nanowire Arrays on Graphene Oxide Sheets with Synergistic Effect for Energy Storage. *ACS Nano* **2010**, *4*, 5019–5026.
28. He, G.; Chen, H.; Zhu, J.; Bei, F.; Sun, X.; Wang, X. Synthesis and Characterization of Graphene Paper with Controllable Properties *via* Chemical Reduction. *J. Mater. Chem.* **2011**, *21*, 14631–14638.
29. Wang, K.; Zou, W.; Quan, B.; Yu, A.; Wu, H.; Jiang, P.; Wei, Z. An All-Solid-State Flexible Micro-Supercapacitor on a Chip. *Adv. Energy Mater.* **2011**, *1*, 1068–1072.
30. Wang, K.; Wu, H.; Meng, Y.; Zhang, Y.; Wei, Z. Integrated Energy Storage and Electrochromic Function in One Flexible Device: An Energy Storage Smart Window. *Energy Environ. Sci.* **2012**, *5*, 8384–8389.
31. Wang, K.; Huang, J.; Wei, Z. Conducting Polyaniline Nanowire Arrays for High Performance Supercapacitors. *J. Phys. Chem. C* **2010**, *114*, 8062–8067.
32. Masarapu, C.; Zeng, H. F.; Hung, K. H.; Wei, B. Effect of Temperature on the Capacitance of Carbon Nanotube Supercapacitors. *ACS Nano* **2009**, *3*, 2199–2206.
33. Dai, L.; Chang, D. W.; Baek, J. B.; Lu, W. Carbon Nanomaterials for Advanced Energy Conversion and Storage. *Small* **2012**, *8*, 1130–1166.
34. Fan, Z.; Yan, J.; Zhi, L.; Zhang, Q.; Wei, T.; Feng, J.; Zhang, M.; Qian, W.; Wei, F.; Three-Dimensional, A. Carbon Nanotube/Graphene Sandwich and Its Application as Electrode in Supercapacitors. *Adv. Mater.* **2010**, *22*, 3723–3728.
35. Miao, M. Yarn Spun from Carbon Nanotube Forests: Production, Structure, Properties and Applications. *Particuology* **2013**, *11*, 378–393.
36. Fan, L. Z.; Hu, Y. S.; Maier, J.; Adelhelm, P.; Smarsly, B.; Antonietti, M. High Electroactivity of Polyaniline in Supercapacitors by Using a Hierarchically Porous Carbon Monolith as a Support. *Adv. Funct. Mater.* **2007**, *17*, 3083–3087.
37. Miao, M. Electrical Conductivity of Pure Carbon Nanotube Yarns. *Carbon* **2011**, *49*, 3755–3761.
38. Ouyang, J.; Chu, C. W.; Chen, F. C.; Xu, Q.; Yang, Y. High-Conductivity Poly(3,4-ethylenedioxythiophene):Poly(styrene sulfonate) Film and Its Application in Polymer Optoelectronic Devices. *Adv. Funct. Mater.* **2005**, *15*, 203–208.
39. Choi, K. S.; Liu, F.; Choi, J. S.; Seo, T. S. Fabrication of Free-Standing Multilayered Graphene and Poly(3,4-ethylenedioxythiophene) Composite Films with Enhanced Conductive and Mechanical Properties. *Langmuir* **2010**, *26*, 12902–12908.
40. Lang, U.; Naujoks, N.; Dual, J. Mechanical Characterization of PEDOT:PSS Thin Films. *Synth. Met.* **2009**, *159*, 473–479.
41. Niu, Z.; Zhou, W.; Chen, J.; Feng, G.; Li, H.; Ma, W.; Li, J.; Dong, H.; Ren, Y.; Zhao, D.; et al. Compact-Designed Supercapacitors Using Free-Standing Single-Walled Carbon Nanotube Films. *Energy Environ. Sci.* **2011**, *4*, 1440–1446.
42. Huynh, C. P.; Hawkins, S. C. Understanding the Synthesis of Directly Spinnable Carbon Nanotube Forests. *Carbon* **2010**, *48*, 1105–1115.
43. Miao, M.; Chen, R. Yarn Twisting Dynamics. *Text. Res. J.* **1993**, *63*, 150–158.
44. Miao, M.; Barnes, S.; Vuckovic, L. High-Speed Video Graphic Study of Filament-Core Yarn Spinning. *J. Text. Inst.* **2009**, *101*, 242–252.
45. Miao, M.; How, Y.-L.; Ho, S.-Y. Influence of Spinning Parameters on Core Yarn Sheath Slippage and Other Properties. *Text. Res. J.* **1996**, *66*, 676–684.
46. Uster Technologies AG: Uster Statistics - Fibre and Yarn Quality. http://www.uster.com/en/service/uster-statistics/ (accessed April 24, 2014).
47. Rahy, A.; Yang, D. J. Synthesis of Highly Conductive Polyaniline Nanofibers. *Mater. Lett.* **2008**, *62*, 4311–4314.
48. Zhai, Y.; Dou, Y.; Zhao, D.; Fulvio, P. F.; Mayes, R. T.; Dai, S. Carbon Materials for Chemical Capacitive Energy Storage. *Adv. Mater.* **2011**, *23*, 4828–4850.
49. Rudge, A.; Davey, J.; Raistrick, I.; Gottesfeld, S.; Ferraris, J. P. Conducting Polymers as Active Materials in Electrochemical Capacitors. *J. Power Sources* **1994**, *47*, 89–107.
50. Miao, M.; McDonnell, J.; Vuckovic, L.; Hawkins, S. C. Poisson's Ratio and Porosity of Carbon Nanotube Dry-Spun Yarns. *Carbon* **2010**, *48*, 2802–2811.